

Tumorigenesis and Neoplastic Progression

A Novel Organotypic Model Mimics the Tumor Microenvironment

Sini Nurmenniemi,^{*†‡} Teemu Sinikumpu,^{*}
Ilkka Alahuhta,^{*} Sirpa Salo,^{**} Meeri Sutinen,^{**}
Markku Santala,[§] Juha Risteli,^{†¶} Pia Nyberg,^{**}
and Tuula Salo^{**¶}

From the Department of Diagnostics and Oral Medicine,^{*} Institute of Dentistry, the Department of Clinical Chemistry,[†] Institute of Diagnostics, and the Oulu Center for Cell-Matrix-Research,[‡] University of Oulu, Oulu; and the Departments of Obstetrics and Gynecology,[§] and Oral and Maxillofacial Surgery,[¶] Oulu University Hospital, Oulu, Finland

Carcinoma cell invasion is traditionally studied in three-dimensional organotypic models composed of type I collagen and fibroblasts. However, carcinoma cell behavior is affected by the various cell types and the extracellular matrix (ECM) in the tumor microenvironment. In this study, a novel organotypic model based on human uterine leiomyoma tissue was established and characterized to create a more authentic environment for carcinoma cells. Human tongue squamous cell carcinoma cells (HSC-3) were cultured on top of either collagen or myoma. Organotypic sections were examined by immunohistochemistry and *in situ* hybridization. The maximal invasion depth of HSC-3 cells was markedly increased in myomas compared with collagen. In myomas, various cell types and ECM components were present, and the HSC-3 cells only expressed ECM molecules in the myoma model. Organotypic media were analyzed by radioimmunoassay, zymography, or Western blotting. During carcinoma cell invasion, matrix metalloproteinase-9 production and collagen degradation were enhanced particularly in the myoma model. To evaluate the general applicability of the myoma model, several oral carcinoma, breast carcinoma, and melanoma cell lines were cultured on myomas and found to invade in highly distinct patterns. We conclude that myoma tissue mimics the native tumor microenvironment better than previous organotypic models and possibly enhances epithelial-to-mesenchymal transition. Thus, the myoma model provides a promising tool for analyzing the behavior of

carcinoma cells. (*Am J Pathol* 2009, 175:1281–1291; DOI: 10.2353/ajpath.2009.081110)

Tumor growth and invasion are not just determined by the malignant tumor cells, but instead various cell types and the extracellular matrix (ECM) of the tumor microenvironment affect the outcome.¹ Particularly, fibroblasts have many prominent roles in the cancer progression. In fact, in many carcinomas, the majority of the stromal cells are fibroblasts that possess myofibroblastic characteristics and are called cancer-associated fibroblasts. They produce ECM molecules, proteases, growth factors, and chemokines that crucially affect the carcinoma cell behavior.^{2,3} In this context, the organotypic three-dimensional skin model developed by Fusenig et al⁴ replicates the *in vivo* situation more closely *in vitro* than the two-dimensional cell culture experiments. The model allows studying of carcinoma cell invasion in three-dimensional collagen gel embedded with fibroblasts. The degree of invasion can also be quantitatively analyzed.^{5,6} However, this kind of organotypic model remains somewhat artificial due to the lack of other cell types besides fibroblasts and ECM components that are present *in vivo*. In addition to the carcinoma cells and fibroblasts, endothelial and inflammatory cells, as well as several ECM molecules, are known to contribute to the tumor growth. The induction of angiogenesis, recruitment of inflammatory cells, and increased turnover of ECM components result in tumor progression.^{7,8} Therefore, we wished to determine whether real human tissue can be used in the organotypic method to

Supported by the Academy of Finland, Finnish Cancer Organizations, Finnish Cultural Foundation, Finnish Dental Society Apollonia, Graduate School of In Vitro Diagnostics, Foundation for Laboratory Medicine, Cancer Foundation of Northern Finland, and research funds from the Medical Faculty of the University of Oulu and Oulu University Hospital special state support for research.

Accepted for publication June 11, 2009.

P.N. and T.S. share equal supervision.

Supplemental material for this article can be found on <http://ajp.amjpathol.org>.

Address reprint requests to Tuula Salo, Department of Diagnostics and Oral Medicine, Institute of Dentistry, PO Box 5281, University of Oulu, FIN-90014 Oulu, Finland. E-mail: tuula.salo@oulu.fi.

provide a more natural stroma-like environment for studying carcinoma cell invasion. We used uterine leiomyoma tissue, which mainly consists of smooth muscle actin (SMA)-positive cells and collagens.⁹ The existence of various additional cell types and proteins in the myoma tissue was characterized, and the invasiveness of malignant human tongue squamous cell carcinoma cells (HSC-3) into this novel myoma organotypic culture was measured by different methods and compared with the traditional collagen organotypic model. To test the general applicability of the myoma model, the invasion patterns of various cell lines were examined in myoma and collagen organotypic cultures.

Materials and Methods

Cell Culture

Human gingival fibroblasts (GF) were obtained from biopsies of healthy gingiva.¹⁰ They were cultured in DMEM supplemented with 100 U/ml penicillin, 100 μ g/ml streptomycin, 50 μ g/ml ascorbic acid, 250 ng/ml fungizone, 1 mmol/L sodium pyruvate (all from Sigma-Aldrich, Ayrshire, UK), and 10% heat-inactivated fetal bovine serum (Perbio Science, Erembodegem, Belgium). Human tongue squamous cell carcinoma cells HSC-3 (JCRB 0623; Osaka National Institute of Health Sciences, Osaka, Japan), human dysplastic oral keratinocytes DOK (European Collection of Cell Cultures 94122104, Salisbury, Wiltshire, UK)¹¹ and human oropharyngeal squamous cell carcinoma (SCC) cells (UK1)^{12,13} were cultured in 1:1 DMEM/F-12 (Invitrogen, Carlsbad, CA) supplemented with 100 U/ml penicillin, 100 μ g/ml streptomycin, 50 μ g/ml ascorbic acid, 250 ng/ml fungizone, 5 μ g/ml insulin (bovine pancreas), 0.4 ng/ml hydrocortisone (all from Sigma-Aldrich), and 10% heat-inactivated fetal bovine serum. Breast adenocarcinoma cell line MDA-MB-231 (ATCC HTB-26) was cultured in HSC-3 media described above. Melanoma cell lines Bowes (ATCC CRL-9607) and G361 (ATCC CRL-1424) were cultured in GF media described above. For the gelatin zymography and Western blotting samples, fetal bovine serum was replaced by 0.5% lactalbumin (Sigma-Aldrich). The cells were cultured in a humidified atmosphere of 5% CO₂ at 37°C and passaged routinely using trypsin-EDTA (Sigma-Aldrich).

Collagen Organotypic Culture

The collagen gel was prepared as previously described⁵ with a few modifications. Briefly, 8 volumes of collagen type I (3.45 mg/ml; BD Biosciences, Bedford, MA), 1 volume of 10 \times DMEM (Sigma-Aldrich), and 1 volume of fetal bovine serum with GF (final concentration in gel 7 \times 10⁵ cells/ml) were mixed on ice. One-milliliter aliquots were allowed to polymerize on 24-well plates at 37°C for 30 minutes. After polymerization, 7 \times 10⁵ cancer cells were added on each gel. Next day the gels were detached from the well walls, allowed to contract for 4 hours and lifted onto collagen-coated (BD Biosciences) nylon disks (Prinsal Oy, Tuusula, Finland) resting on curved steel grids (3 \times 21 \times 21 mm). The grids were placed on

6-well plates, and a sufficient volume of culture media (2.5 ml) was added to reach the undersurface of the grid generating an air-liquid interface. This was day 1 of the culture. In the inhibition assays, matrix metalloprotease (MMP) inhibitor GM6001 (Chemicon International, Temecula, CA) was added to the culture media at 5 and 100 μ mol/L concentrations. The media of the organotypic cultures were collected and changed every 3 days. The cultured tissues were harvested at days 2, 8, and 14. The collected media were stored at -20°C.

Myoma Organotypic Culture

Uterine leiomyoma tissue was obtained from routine surgical operations after informed consent of the donors. The study was approved by the Ethics Committee of the Oulu University Hospital. Only nondegenerated myomas were selected for the study. To prepare myoma disks for the organotypic culture, the tissue was cut into 3-mm slices with a disposable scalpel and further into disks with an 8-mm biopsy punch (Kai Industries Co., Gifu, Japan). Macroscopically heterogeneous areas of the myoma tissue were omitted. The myoma disks were stored at -70°C in media with 10% DMSO (Sigma-Aldrich). As there are differences between myoma tissues, each experiment was done using disks from the same myoma. To prepare myoma-based organotypic cultures, myoma disks were equilibrated in media at room temperature for 1 hour. The myoma disks were placed into Transwell inserts (diameter, 6.5 mm; Corning, Inc., Corning, NY), and 7 \times 10⁵ cancer cells in 50 μ l of media were added on top of each myoma disk. The cells were allowed to attach overnight, and the myoma disks were removed from the Transwell inserts and transferred onto uncoated nylon disks resting on curved steel grids (3 \times 12 \times 15 mm) in 12-well plates with sufficient volume of media (1 ml). The myoma organotypic cultures were maintained, and the media changed according to the collagen organotypic culture protocol described above.

Histology and Immunohistochemistry

At days 2, 8 and 14, the organotypic cultures were fixed in 4% neutral-buffered formalin overnight. The specimens were dehydrated, bisected, and embedded in paraffin. Sections (6 μ m) were deparaffinized and stained with Mayer's H&E. For immunohistochemistry of pancytokeratin AE1/AE3, Ki-67, carboxyterminal telopeptide of type I collagen (ICTP), amino-terminal telopeptide of type III collagen, collagen IV, laminins, vimentin (VIM), SMA, CD45, CD68, and factor VIII antibodies, the endogenous peroxidase activity was blocked with 0.3% H₂O₂ in MeOH for 30 minutes. Antigen retrieval was performed by 0.4% pepsin in 0.01 M HCl at 37°C for 1 hour or by microwaving (T/T Mega; Milestone, Bergamo, Italy) the sections in citrate buffer (REAL Target Retrieval Solution, pH 6; Dako, Glostrup, Denmark) or in Tris/EDTA (10 mmol/L Tris, 1 mmol/L EDTA, pH 9) for 20 minutes. Sections were blocked with normal serum (Vector Laboratories, Burlingame, CA) in 2% bovine serum albumin/

Table 1. Primary Antibodies Used for Immunohistochemistry

Antibody	Species	Clone	Antigen retrieval	Dilution	Source
Cytokeratin	Mouse	AE1/AE3	Tris/EDTA	1:150	Dako
Ki67	Mouse	MM1	Citrate	1:100	Novocastra Laboratories Ltd. (Newcastle upon Tyne, UK)
ICTP	Rabbit	Poly	Citrate	1:500	(18)
IIINTP	Rabbit	Poly	Citrate	1:50	(32)
Collagen IV	Mouse	CIV 22	Citrate	1:100	Dako
Laminins	Rabbit	Poly	Pepsin	1:600	Dako
Vimentin	Mouse	Vim 3B4	Tris/EDTA	1:1500	Dako
SMA	Mouse	1A4	Tris/EDTA	1:1000	Dako
CD45	Mouse	2B11, PD7/26	Tris/EDTA	1:400	Dako
CD68	Mouse	PG-M1	Tris/EDTA	1:200	Dako
Factor VIII	Rabbit	Poly	Tris/EDTA	1:5000	Dako
E-cadherin	Rabbit	Poly	Citrate	1:50	Cell Signaling Technology (Beverly, MA)
S100	Rabbit	Poly	Tris/EDTA	1:3000	Dako

ICTP, carboxyterminal telopeptide of type I collagen; IIINTP, amino-terminal telopeptide of type III collagen.

PBS for 30 minutes and then incubated with primary antibodies in a humidified chamber at 37°C for 30 minutes and at 4°C overnight. Dilutions were prepared in REAL Antibody Diluent (Dako). Biotinylated secondary antibody of appropriate species (Vector Laboratories) was applied for 1 hour and StreptABComplex/HRP (Dako) in 0.5 M NaCl/PBS was applied for 30 minutes. After each step, the sections were washed twice in PBS for 10 minutes. S100 and E-cadherin were stained with REAL EnVision Detection System (Dako) according to the manufacturer's instructions. S100 was incubated at room temperature for 30 minutes and E-cadherin at 4°C overnight, and the secondary antibody was applied for 30 minutes. The information of the primary antibodies is shown in Table 1. The presence of antigen was visualized using 3,3'-diaminobenzidine (brown; Vector) for 3 minutes or aminoethyl carbazole (red; Invitrogen) for 10 minutes. 3,3'-Diaminobenzidine - and aminoethyl carbazole-stained sections were counterstained with Mayer's hematoxylin and mounted with xylene or Aquatex (Merck, Dannstadt, Germany), respectively. In negative controls, normal serum or IgG of appropriate species (Dako) was used instead of primary antibody.

Quantification of Invasion

AE1/AE3-immunostaining was performed to identify carcinoma cells. Sections were digitally recorded at ×100 magnification with a DMRB photo microscope connected to a DFC 480 camera using QWin V3 software (all from Leica Microsystems, Heerbrugg, Switzerland). The areas of immunostained noninvading and invading cells were calculated, excluding the nonuniform invasion in the edges of the gel and myoma. Any artifactual invasion, which occurred occasionally in clearly identifiable areas where the myoma tissue structure was less dense than

normally, was also omitted. The invasion index ($1 - [\text{non-invading area}/\text{total area}]$) was calculated as previously described,⁶ and the maximal invasion depth per microscopic field (the distance of the deepest invading cell from the lower surface of the noninvasive cell layer) was measured in each sample.

Quantification of Proliferation

Cell proliferation rate was determined as percentage of Ki-67-expressing cells among all carcinoma cells (at least 100 cells) per microscopic field. Three fields per collagen gel or myoma sample were counted, at ×200 magnification.¹⁴

In Situ Hybridization

In situ hybridization was performed as previously described¹⁵ in 6-μm paraffin-embedded collagen and myoma organotypic sections. Human cDNA fragments used for probe preparation are described in Table 2. The vectors were linearized with suitable enzymes and the transcripts were labeled with digoxigenin-11-UTP (DIG RNA labeling kit; Roche Diagnostics GmbH, Mannheim, Germany). Corresponding sense probes were used as controls for nonspecific hybridization. *In situ* hybridization was performed at probe concentration of 300 to 400 ng/ml.

Zymography

The organotypic serum-free conditioned media samples collected every 3 days were concentrated 1:4. Gelatin zymography was performed as described previously.¹⁶

Table 2. Human cDNA Probes Used for *in Situ* Hybridization

Probe	Size (bp)	Transcription vector	Restriction sites	Reference
Proα1(I) coll	372	pGEM1	PstI-PvuII	(33, 34)
Proα1(III) coll	379	pGEM1	PstI-PstI	(35)
α1(IV) coll	916	pSP64 and pSP65	BamHI-HindIII	(36)
Laminin-332 γ2	845	pSP64 and pSP65	PstI-EcoRI	(37)

Western Blotting

The organotypic serum-free conditioned media samples collected every 3 days were concentrated 1:4 and analyzed by Western blotting. Briefly, the samples were separated on a 12% SDS-PAGE under reducing conditions and electrotransferred to an Immobilon-P polyvinylidene difluoride membrane (Millipore, Bedford, MA). Nonspecific binding was blocked with 5% nonfat dry milk for 1 hour, and the membranes were probed with polyclonal rabbit anti-MMP-1 C-terminus (1:1000; Millipore/Chemicon International, Billerica, MA), polyclonal goat anti-MMP-8 (1:200; Santa Cruz Biotechnology, Heidelberg, Germany), or monoclonal mouse anti-MMP-13 (1:500; Oncogene, San Diego, CA) overnight, followed by a biotinylated secondary antibody (Dako). The immunoreactive proteins were visualized with Vectastain Elite ABC Kit detection reagents (Vector Laboratories) according to manufacturer's instructions.

Analysis of Collagen Metabolites by Radioimmunoassays

Polyclonal antibodies against the synthetic peptide SP99 (GGVGAAlAGIGGEKAGGFAPY; NeoMPS, Strasbourg, France) from the carboxyterminal telopeptide of type III collagen (IIICTP) were raised in rabbits. Antiserum was appropriately diluted for the SP99-radioimmunoassay (RIA). SP99 was labeled with ^{125}I by the Chloramine-T method.¹⁷ Aliquots (100 μl) of myoma organotypic media samples (diluted 1:2–1:20 to adjust the sample concentration to the standard curve range) were incubated with 200 μl of the antiserum dilution and 200 μl of ^{125}I -antigen solution at 37°C for 2 hours. After that, 500 μl of the second antibody in 10% polyethylene glycol (6 kDa) was added, and the samples were incubated at 4°C for 30 minutes. The samples were centrifuged at 2000 $\times g$ at 4°C for 30 minutes, and the radioactivity in the precipitates was counted with a gamma counter (1470 Wallac Wizard; GMI, Ramsey, MN). The ICTP¹⁸ was measured using commercially available ICTP-RIA according to manufacturer's (Orion Diagnostica Oy, Espoo, Finland) instructions.

Statistical Analysis

SPSS 16.0 (SPSS, Inc., Chicago, IL) was used for calculations. The invasion and proliferation results are represented in box plots as median [25th percentile, 75th percentile]. The whiskers mark the data points within 1.5 interquartile ranges from the median, and the outliers are indicated. The independent samples *t*-test was used for determining the statistical significance of differences. Mann-Whitney *U*-test was used for the data not conforming to a normal distribution. The RIA results are represented as mean \pm SE.

Results

Carcinoma Cell Invasion Depth Is Enhanced by the Myoma Tissue

To study the invasive behavior of HSC-3 oral carcinoma cells at different time points (days 2, 8, and 14), transverse sections of collagen and myoma organotypic cultures were stained with anti-pancytokeratin AE1/AE3 (Figure 1A). Cytokeratin is an epithelial cell marker and thus identifies the epithelium-derived HSC-3 carcinoma cells. To quantify the invasion of HSC-3 cells at day 14, the maximal invasion depth (Figure 1B) and the invasion area (Figure 1C) per microscopic field were measured both in collagen and myoma organotypic cultures, and the invasion index was determined (Figure 1D). The growth of HSC-3 cells was different depending whether the cells were growing on top of collagen or myoma. The carcinoma cells formed a thick cell layer on top of myoma, but on collagen, the cells grew as a single-cell layer. We also observed that the invasion patterns were different; in collagen, the carcinoma cells invaded as an invasive front or in chain-like fashion but in myoma more as individual cells or small clusters. In myoma, the average maximal invasion depth of carcinoma cells was 8.2-fold (547 [507, 568] μm) in comparison with collagen (67 [59, 83] μm) (Figure 1B). In many myomas, the invasion continued beyond the depth that could be measured per microscopic field, and thus, the difference in maximal invasion depth may even be bigger. The invasion areas were almost the same in both cultures (34,532 [30,214, 41,387] μm^2 in collagen and 36,710 [25,632, 51,134] μm^2 in myoma) (Figure 1C). However, because of the differences in the growth patterns, the invasion index was higher in collagen organotypic cultures (0.75 [0.73, 0.80]) than in myoma organotypic cultures (0.51 [0.41, 0.60]) (Figure 1D).

Carcinoma Cell Proliferation in Collagen Gel and Myoma Tissue

The effect of the organotypic matrix on the carcinoma cell proliferation was studied by immunostaining the collagen and myoma organotypic cultures for proliferation marker Ki-67 (Figure 2A). The percentage of Ki-67-positive carcinoma cells out of total cell number per microscopic field was calculated. In collagen organotypic culture, the proliferation rate at day 14 was 2.7-fold (19.0 [12.8, 23.7] %) in comparison with myoma organotypic culture (7.0 [4.7, 15.8] %) (Figure 2B).

Myoma Tissue Mimics Tumor Microenvironment

To determine which components in the myoma organotypic culture could be responsible for enhancing the carcinoma cell invasion depth, the cultures were immunostained for various proteins and cell markers. Myoma tissue was shown to contain ECM proteins, such as collagens type I and III (Figure 3, A and B, respectively), and basement membrane proteins, such as collagen type IV

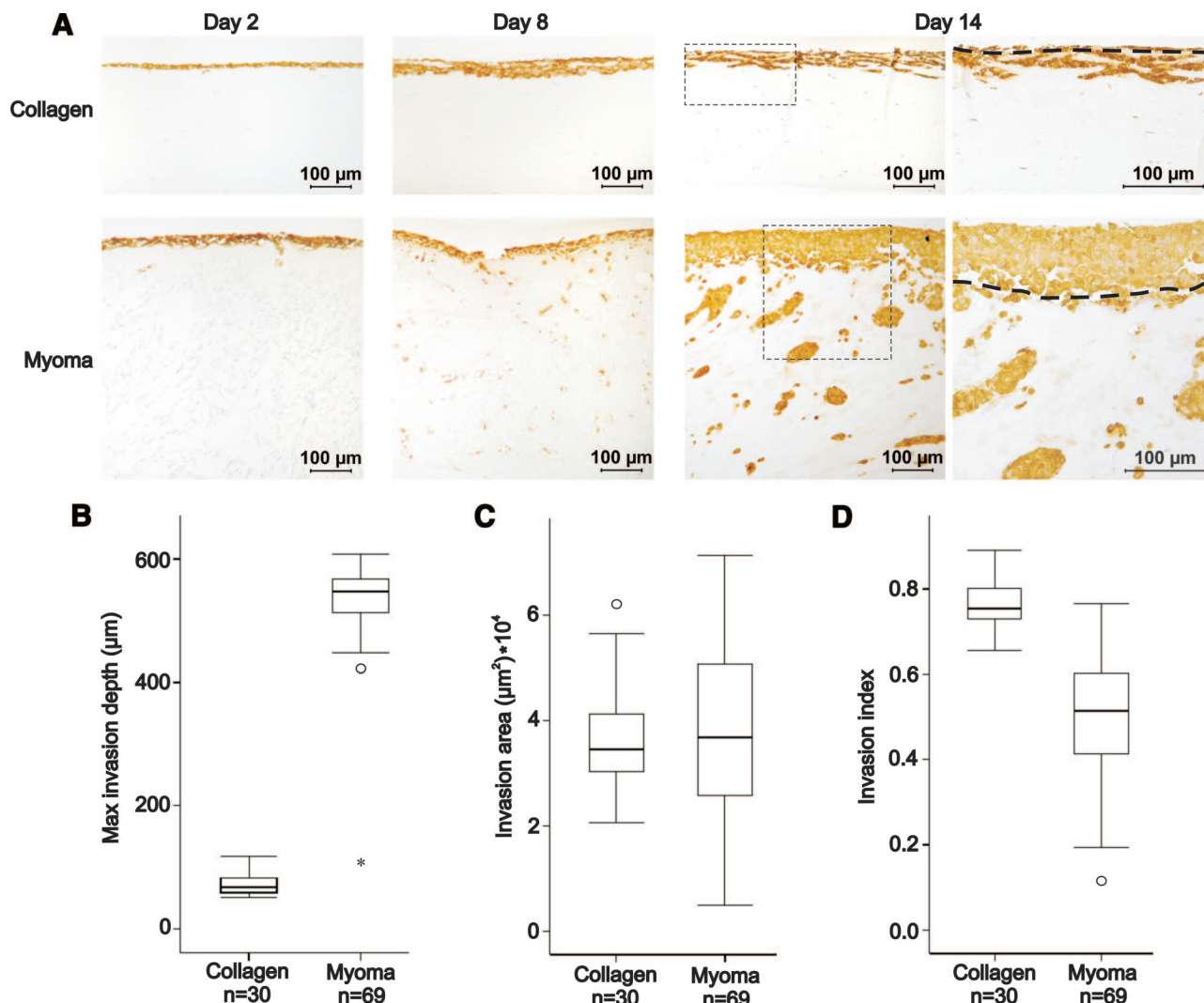


Figure 1. Carcinoma cell invasion into collagen and myoma organotypic cultures. HSC-3 cells (7×10^5) were cultured on top of type I collagen gel embedded with GF (7×10^5) or on top of myoma tissue. At days 2, 8, and 14, the cultures were formalin-fixed, processed to paraffin blocks, sectioned, and stained with anti-pancytokeratin AE1/AE3 (A), which stains the epithelial-derived carcinoma cells brown. Original magnifications $\times 100$ (days 2, 8 and 14) and $\times 200$ (day 14, the panels on the right are higher magnifications from the boxed areas in the panels on the left). The dashed line (day 14) represents the lower surface of the noninvasive cell layer. Scale bar, 100 μm . The cytokeratin-positive areas were quantified with QWin V3 software. The difference in invasion at day 14 between collagen and myoma organotypic cultures was quantified as maximal invasion depth (the distance from the lower surface of the noninvasive cell layer to the deepest invaded cell) (Mann-Whitney U -test, $P = 0.000$) (B), invasion area (t -test, $P = 0.595$) (C), and invasion index ($1 - [\text{noninvasive area}/\text{total area}]$) (t -test, $P = 0.000$) (D). The results consist of at least three measurements of two to eight replicates from two to four independent assays.

and laminins (Figure 3, C and D, respectively). These ECM and basement membrane components seem to be more intensively stained around the carcinoma cell islands as well as under the carcinoma cell surface (Figure 3, A–D), which suggested that the carcinoma cells were producing these matrix molecules. This was confirmed by *in situ* hybridization, which revealed that in the myoma model the HSC-3 carcinoma cells expressed mRNA for procollagens I and IV, and laminin-332 $\gamma 2$ -chain (Figure 3, E–G, respectively). In the collagen model, the expression of these molecules was almost undetectable (not shown). Myoma tissue was also demonstrated to contain various cell types, such as fibroblasts (VIM and SMA), smooth muscle cells (SMA), lymphocytes (CD45), macrophages (CD68), and endothelial cells (Factor VIII) (Figure 3, H–L, respectively), which makes it a more natural stroma-like environment

compared with the collagen organotypic culture. To show that the carcinoma cells did not induce any changes in the myoma tissue proteins or cell types, native myomas were cultured in the absence of HSC-3 cells (Supplemental Figure S1, see <http://ajp.amjpathol.org>). Negative IgG controls for monoclonal and polyclonal antibodies are shown in Supplemental Figure S2 (see <http://ajp.amjpathol.org>).

Interestingly, some carcinoma cells stained positively for the mesenchymal marker VIM (Figure 3H), suggesting that these cells might be going into epithelial-to-mesenchymal transition (EMT). To study this in detail, serial sections were stained with VIM (Figure 4A, red) and the epithelial marker pancytokeratin AE1/AE3 (Figure 4B, brown). In addition, a double staining with VIM (red) and AE1/AE3 (blue) was performed (Figure 4C). In Figure 4, A–C, the arrows point out representative carcinoma cells

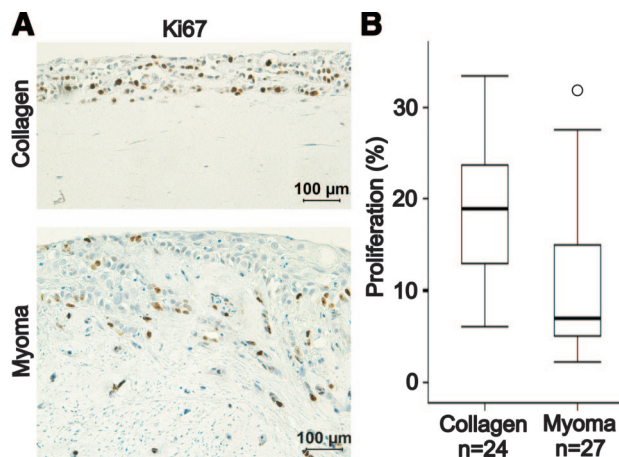


Figure 2. HSC-3 carcinoma cell proliferation in collagen and myoma organotypic cultures. **A:** Paraffin-embedded 14-day collagen and myoma organotypic sections were stained for proliferation marker Ki-67. Scale bar, 100 μ m. **B:** Proliferation was defined as percentage of stained HSC-3 cells of all HSC-3 cells per microscopic field in eight collagen gel or nine myoma samples (three fields per sample) that were pooled from at least five independent assays (*t*-test, *P* = 0.001).

clearly expressing both the mesenchymal and epithelial markers.

Carcinoma Cells Induce Matrix Remodelling in Myoma Tissue

To study the effect of invasion on ECM degradation, the presence of collagen degradation products in the conditioned media samples of myoma organotypic cultures was determined by radioimmunoassay. ICTP assay measures type I collagen degradation and SP99-assay type III collagen degradation. As the invading carcinoma cells degrade collagens, these assays could be a quantitative tool to measure invasion in human tissue. When carcinoma cells were present on top of myoma tissue, both type I and type III collagen degradation increased until day 11 and reached a plateau after that (Figure 5, A and B). In the absence of carcinoma cells, the level of the collagen degradation was the same as in the presence of cells at the beginning, but it gradually decreased from day 4 forward.

Since MMPs play an important role in degrading ECM and basement membranes, the production of gelatinases (MMP-2 and MMP-9) and collagenases (MMP-1, MMP-8, and MMP-13) into conditioned organotypic media was determined by gelatin zymography or Western blotting. The normal organotypic media was modified by omitting serum, which slightly decreased invasion in the myoma and significantly inhibited invasion in the collagen. Figure 6A illustrates that in myoma organotypic cultures the amounts of latent and active MMP-9 were dramatically increased during the carcinoma cell invasion (day 4 in lane 7, compared with day 14 in lane 8). In collagen organotypic cultures, only moderate amounts of pro-MMP-9 were detected (lanes 5–6). When carcinoma cells

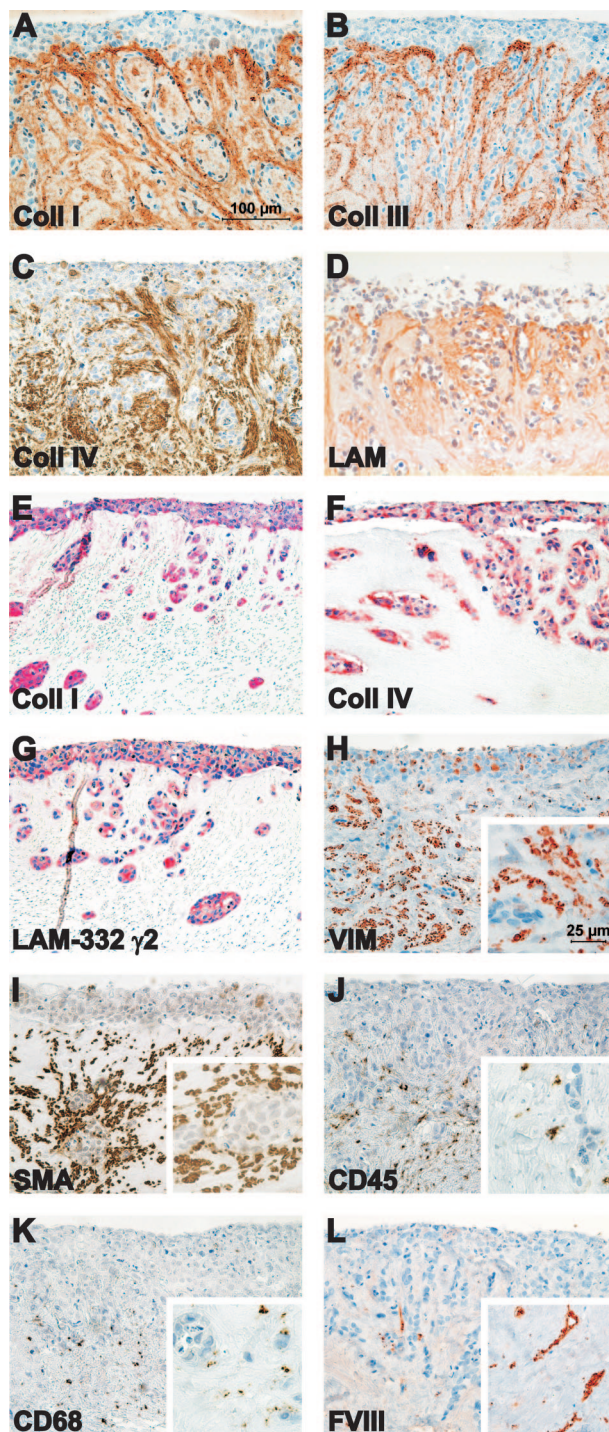


Figure 3. Characterization of the myoma organotypic culture. HSC-3 cells were cultured on top of myoma tissue, and the 14-day paraffin embedded sections were immunostained for type I collagen (anti-ICTP) (A), type III collagen (anti-N-terminal telopeptide of type III collagen) (B), type IV collagen (C), and laminins (D). The mRNAs for type I procollagen (E), type IV procollagen (F), and laminin-332 γ 2-chain (G) were detected in carcinoma cells in myoma organotypic cultures by *in situ* hybridization. The myoma organotypic cultures were also immunostained for fibroblasts (anti-VIM) (H), smooth muscle cells and myofibroblasts (anti-SMA) (I), lymphocytes (anti-CD45) (J), macrophages (anti-CD68) (K), and endothelial cells (anti-factor VIII) (L). Scale bar: 100 μ m, in higher magnification insets (H–L) 25 μ m.

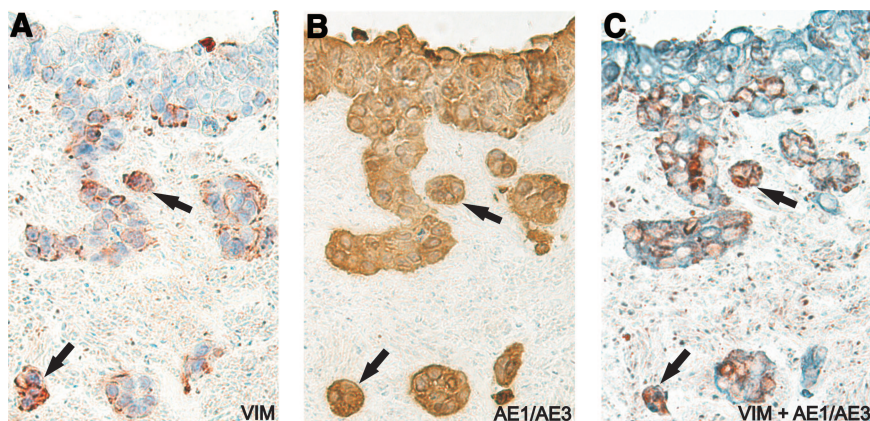


Figure 4. Colocalization of VIM and pancyokeratin in HSC-3 carcinoma cells. HSC-3 cells were cultured on top of myoma tissue, and the 14-day paraffin-embedded sections were immunostained with a mesenchymal marker VIM (red) (A), an epithelial marker pancyokeratin (AE1/AE3, brown) (B), and both VIM (red) and pancyokeratin (blue) (C). The arrows indicate representative HSC-3 cells positive for both of these markers. Original magnification, $\times 200$.

were not present, only MMP-2 production was observed (lanes 1–4). This suggests that the HSC-3 cells are the main producers of MMP-9, and the fibroblasts and the myoma tissue are the main sources of MMP-2. The proportion of active MMP-2 was higher in myoma organotypic culture (lanes 3–4 and 7–8), although active and pro-MMP-2 were present in both cultures. Western blotting of MMP-1 (Figure 6B) showed that its secretion was very different into collagen and myoma media: only in collagen, the presence of HSC-3 cells induced MMP-1 production (lanes 1–2 and 5–6). Western blotting of

MMP-8 (Figure 6C) and MMP-13 (Figure 6D) illustrates that significantly more collagenases were present in myoma-conditioned media than in collagen media, but their amount gradually decreased during the experiment. The presence of HSC-3 cells did not affect the amounts of these collagenases, indicating that fibroblasts and myoma tissue are the principal sources.

To evaluate the role of MMPs on myoma tissue remodeling, a broad spectrum MMP-inhibitor GM6001 was added to the organotypic culture media and a large number of serial histological sections were analyzed. As shown in Figure 7A, the invasion of carcinoma cells into the myoma tissue was clearly diminished at 5 $\mu\text{mol/L}$

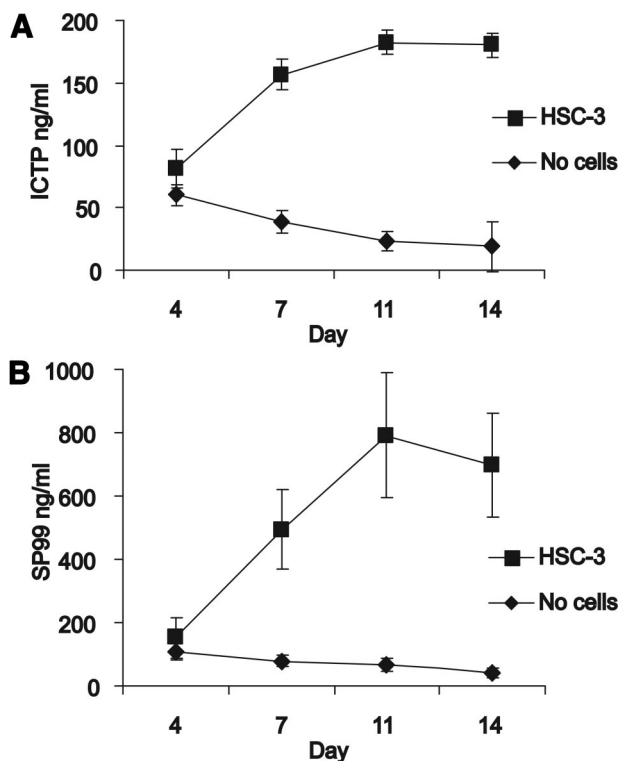


Figure 5. Measurement of collagen metabolites in the conditioned media of myoma organotypic cultures by RIA. The myoma tissue was cultured in the absence and presence of carcinoma cells (HSC-3), and the media were collected at days 4, 7, 10 and 14. **A:** The amount of the ICTP in the media was measured by a commercially available radioimmunoassay. **B:** The amount of IICTP was determined by a novel RIA based on a synthetic peptide (SP99) from the C-terminus of type III collagen. The values shown are the mean of eight replicates (\pm SE) from one representative assay.

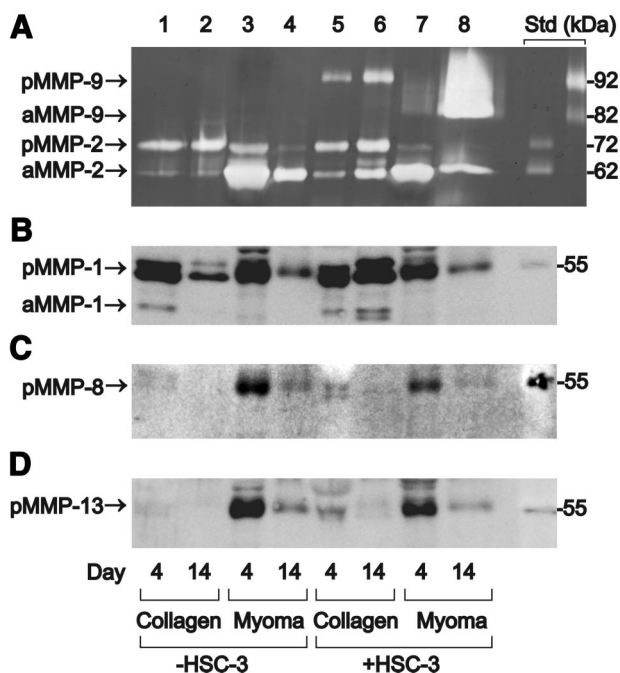


Figure 6. Gelatinases and collagenases in the serum-free conditioned media of organotypic cultures. The collagen and myoma organotypics were cultured in the absence (–) or presence (+) of carcinoma cells (HSC-3), and the media were collected every 3 days (days 4 and 14 shown) and concentrated. **A:** Gelatin zymography for MMP-2 and MMP-9. Purified gelatinase standards are shown on the right: pro-MMP-2 (72 kDa), active MMP-2 (62 kDa), pro-MMP-9 (92 kDa), and active MMP-9 (82 kDa). Western blotting for MMP-1 (latent 52 kDa and active 41 kDa) (B), (C) for MMP-13 (latent 60 kDa), and (D) MMP-8 (latent 54 kDa). Protein molecular weight standards (55 kDa) are shown on the right in B–D.

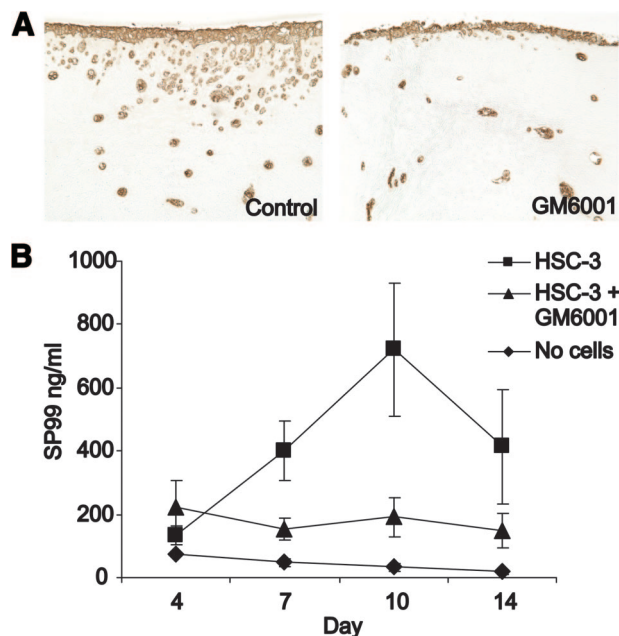


Figure 7. Effect of MMP inhibitor GM6001 on oral carcinoma cell invasion in myoma organotypic cultures. The myoma tissue was cultured with HSC-3 cells in the absence or presence of 5 $\mu\text{mol/L}$ GM6001, and the media were collected at days 4, 7, 10, and 14. **A:** Paraffin-embedded 14-day myoma organotypic sections were stained for pancytokeratin AE1/AE3 to visualize the carcinoma cell invasion. Original magnification, $\times 100$. **B:** The amount of IICTP in the media was determined by a novel RIA based on a synthetic peptide (SP99) from the C-terminus of type III collagen. The values shown are the mean of five or six replicates (\pm SE) from two independent assays.

concentration. The RIA analysis of the type III collagen degradation showed reduced amounts of degradation products confirming the inhibition of invasion (Figure 7B). The invasion was completely blocked with 100 $\mu\text{mol/L}$ GM6001 (not shown). The same kind of phenomena was observed in collagen organotypic cultures (not shown).

Myoma Tissue Enhances Invasion of Various Cell Types

To demonstrate the general applicability of the myoma model, the behavior of various different cell lines was monitored in the organotypic models. A dysplastic oral keratinocyte (DOK), an oral carcinoma (UK1), a breast carcinoma (MDA-MB-231), and two melanoma (Bowes and G361) cell lines were cultured in the organotypic models in addition to the HSC-3 tongue carcinoma cell line. The different invasion patterns are more clearly visible in the myoma model than in the collagen organotypic model, and the myoma tissue seems to significantly enhance the invasion of all cell lines (Figure 8, A–F).

Discussion

As carcinoma cell behavior is highly dependent on the stromal interactions, we wished to develop an organotypic model that would mimic the real human tumor microenvironment better than the traditional organotypic models. The previous models are based on embedding

human fibroblasts into rat type I collagen or mouse EHS tumor-derived basement membrane matrix (Matrigel; BD Biosciences). We examined whether human uterine leiomyoma tissue would be suitable for organotypic cultures. Previously it has been shown that carcinoma cell invasion can be increased by adding fibroblasts or Matrigel into type I collagen.⁵ Thus, increasing the diversity of the organotypic matrix enhances the carcinoma cell invasion. The importance of fibroblasts was highlighted also by our observation that the malignant HSC-3 cells were not able to invade into the fibroblast-free collagen matrix even after 2 months (not shown). The origin and location of fibroblasts are crucial for invasion; only species-specific fibroblasts in contact with SCC cells trigger the invasion^{6,14} by providing pathways for SCC cells through the ECM.⁶ However, since the addition of Matrigel to collagen enhances the invasion, also the composition of the tumor microenvironment seems to be crucial for the invasion. In the myoma tissue, both laminins and collagens (type I, III, and IV) were present, thus participating in the invasive process. Gaggioli et al⁶ have shown that the carcinoma cells particularly like to invade via tracks of collagen and other matrix molecules. The structures in the myoma tissue seem to provide such ECM-rich tracks and thus have an invasion promoting quality. However, it remains to be further studied whether the preformed tracks are one of the most crucial factors in invasion or whether the stromal cells have additional important roles.

The average invasion depth of SCC cells varies in organotypic cultures, being approximately 100 μm , but it can increase up to 600 μm largely depending on the composition of the matrix.^{5,6,14} We found that the myoma-based model seemed to enhance invasion in terms of maximal invasion depth; carcinoma cells invaded over 550 μm in the myoma model in comparison with 70 μm in the collagen model. The widely used invasion indexes suit well when comparing results within the same organotypic model. However, the cell behavior is very different in the two models, and thus the invasion indexes are not comparable. Apparently the diversity of myoma tissue induces the carcinoma cells to grow as characteristic thick epithelial layers. In fact, the invasion pattern of HSC-3 cells in myoma tissue was strikingly similar to invasion pattern of oral SCC cells (H357) in collagen organotypics transplanted in nude mice.⁵ When comparing oral cell lines (HSC-3, DOK, and UK1), the distinct invasion patterns were clearly visible in myoma but not in collagen. Additional cell lines of different origin (breast carcinoma and melanomas) also showed varying degree of invasiveness in myoma, suggesting that the myoma model has general applicability. Furthermore, the Bowes cell line was established from a metastatic melanoma,^{19,20} whereas the G361 cell line was established from a primary nonmetastatic melanoma^{20,21}; their clearly distinct behavior in the myoma model seems to well reflect the invasive capacity of the cells. Similar phenomena can be seen with the oral cell lines that have varying metastatic potential. The HSC-3 cells are known to be very aggressive,²² whereas dysplastic/early neoplastic DOK cell are less invasive,¹¹ and the invasiveness of the UK-1

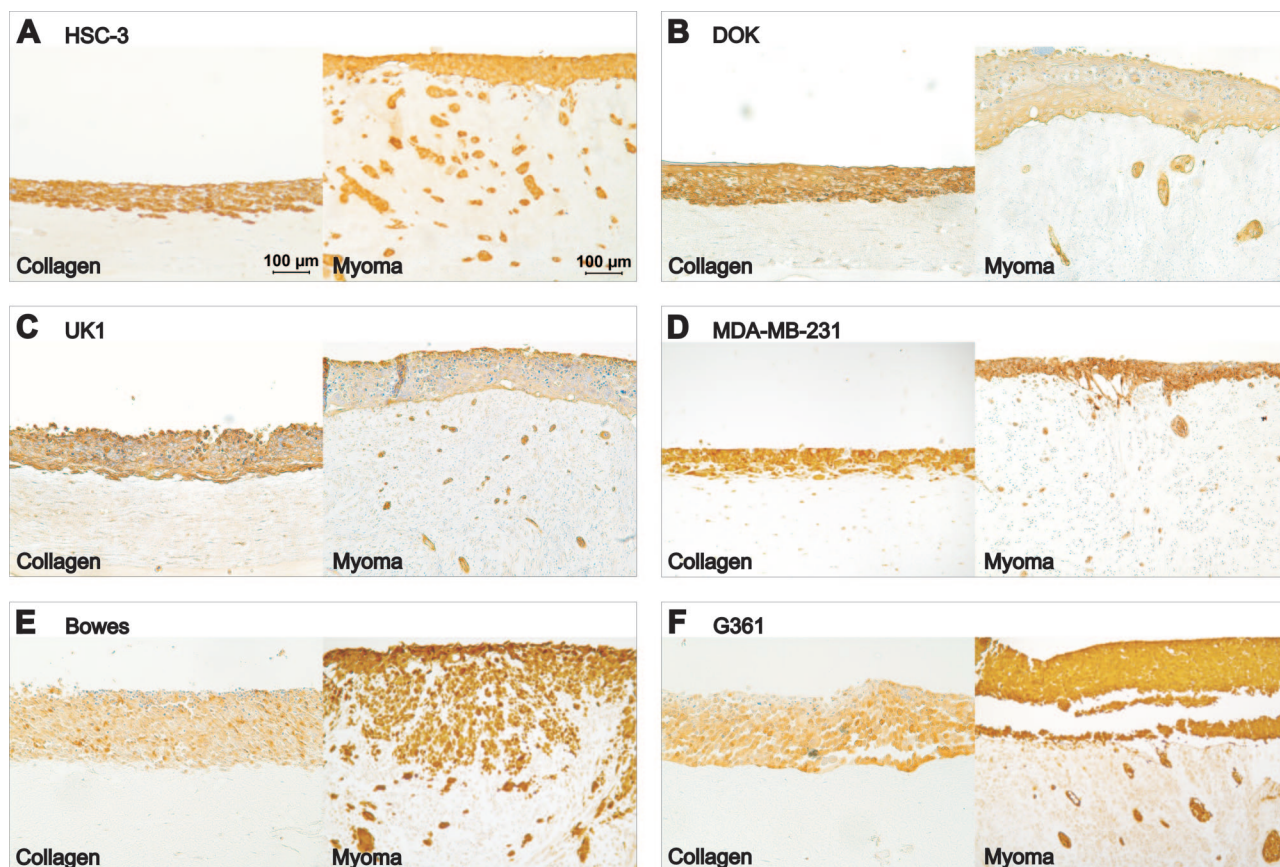


Figure 8. Invasion of different cell types in organotypic cultures. Carcinoma or melanoma cells (7×10^5) were cultured on top of type I collagen gel embedded with GF (7×10^5) or on top of myoma tissue. Paraffin-embedded 14-day collagen and myoma organotypic sections were immunostained to visualize the cells. Tongue carcinoma cells HSC-3 (A), dysplastic oral keratinocytes DOK (B), and oral carcinoma cells UK1 (C) were stained for pancytokeratin AE1/AE3. D: Breast adenocarcinoma cells MDA-MB-231 were stained for E-cadherin. Melanoma cell lines Bowes (E) and G361 (F) were stained for S100. Scale bar: 100 μ m.

cells seems to fall in-between of these other two oral cell lines.

Inflammatory cells, especially macrophages, stimulate angiogenesis and ECM breakdown and thereby promote tumor progression.²³ Angiogenesis is also known to be crucial for tumor growth.²⁴ We detected both macrophages and lymphocytes in the myoma as well as some endothelial cells positive for factor VIII immunostaining. Therefore, the presence of fibroblasts, smooth muscle, endothelial, and inflammatory cells in the myoma tissue is evident to enhance the invasion of oral carcinoma cells. Unexpectedly, the proliferation rate of the HSC-3 cells was higher in the collagen model. However, the lower carcinoma proliferation rate in the myoma model suggests that in the myoma the cells had a more migratory than proliferatory phenotype mimicking the highly invasive oral SCCs *in vivo*. In this context, the invasion depth is an important parameter in determining the malignancy, and the invasion index based only on carcinoma cell areas does not completely reflect the carcinoma aggressiveness.

The ECM can have dual roles in carcinoma progression; on one hand, the ECM molecules form physical barriers that the invading cells need to break, but on the other hand, it provides attachment surfaces and pathways for the invading carcinoma cells⁶ and promotes

EMT.²⁵ We observed here that a portion of the carcinoma cells gained VIM positivity both in myoma (Figures 3H and 4) and collagen models (not shown). VIM is a mesenchymal marker, and its expression by carcinoma cells suggests ongoing EMT possibly induced by the three-dimensional environment. In addition, type I collagen was expressed only by the carcinoma cells growing in the myoma (Figure 3E). Type I collagen induces EMT in lung cancer cells,²⁵ and its expression is considered to be another mesenchymal marker.²⁶

MMPs are a family of proteases that are implicated in cancer²⁷ and can have both protective and destructive roles. The stroma seems to be able to regulate the MMP production. MMP-9 expression is up-regulated in malignant HaCaT tumor cells when they are in contact with stromal fibroblasts *in vitro*.²⁸ We found that the amount and activity of MMP-9 was increased by HSC-3 cells on the myoma stroma in contrast to the collagen gel. On the other hand, the carcinoma cells can also affect the stroma, so the increase in MMP-9 can alternatively be due to HSC-3 cells inducing the MMP-9 production in the stroma. In the collagen organotypic cultures, the amount of MMP-1 was increased by the presence of HSC-3. However, this increase did not happen in the myoma. There was more MMP-8 and MMP-13 present in the myoma culture media than in the collagen organotypic me-

dia, although the carcinoma cells did not seem to be the source of these collagenases. Interestingly, it was found that in the myoma model the presence of carcinoma cells seemed to decrease the presence of MMP-1, MMP-8, and MMP-13. Particularly, the decreased amount of MMP-8 could be biologically important, as MMP-8 has been shown to have a protective role in tongue cancer.²⁹ It is thus possible that during the invasion process the SCC cells might be able to eliminate MMP-8 in their microenvironment.

Since the invasive cells, including HSC-3 cells, have been shown to degrade collagens,³⁰ the presence of collagen degradation products in the organotypic culture media was monitored. By human-specific ICTP-RIA,¹⁸ the degradation of human type I collagen in myoma tissue was confirmed. Similarly, type III collagen degradation in myoma tissue was detected during the cell invasion. To detect the importance of MMPs in the degradation process, a broad-spectrum MMP inhibitor GM6001 was added to the organotypic culture media. GM6001 (5 μ mol/L) clearly decreased the invasion visualized by immunohistochemistry. This correlated with the decreased amount of collagen degradation products measured by RIA (Figure 7). The collagen degradation thus seems to reflect the degree of invasion and could possibly be used to monitor the invasive process. In collagen organotypic cultures, the degradation products could not be observed due to species-specificity of the RIA analysis. Clinically, the ICTP-RIA is used in serum samples, for example, to monitor the MMP-mediated pathological degradation of bone collagen due to metastases of breast, lung, and prostate cancer.³¹

In summary, we have developed and characterized a new improved organotypic culture model based on human myoma tissue. Myoma clearly enhances the invasion depth of many human cancer cell lines originating from various tissues and possibly promotes carcinoma cell EMT. In addition, RIA measurement of collagen degradation products from organotypic cell culture media seems to be a valid method to quantify invasion of tongue carcinoma cells. Thus, the myoma model provides a biologically relevant human matrix for SCC invasion studies.

Acknowledgments

We thank Sanna Juntunen, Eeva-Maija Kiljander, Katja Koukkula, Maija-Leena Lehtonen, Mirja Mäkeläinen, and Merja Tyynismaa for expert technical assistance, Risto Bloigu for statistical advice, Mika Kihlström for help with figure preparation, Riitta Vuento for histological advice, and Daniela Costea, Maria Nyström, and Gareth Thomas for advice in organotypic culture procedures. DOK cells were a generous gift from Daniela Costea, UK1 cells from Ian Mackenzie, MDA-MB-231 cells from Petri Lehenkari, and Bowes and G361 cells from Jorma Keski-Oja.

References

1. Nyberg P, Salo T, Kalluri R: Tumor microenvironment and angiogenesis. *Front Biosci* 2008, 13:6537–6553

2. Kalluri R, Zeisberg M: Fibroblasts in cancer. *Nat Rev Cancer* 2006, 6:392–401
3. Orimo A, Weinberg RA: Stromal fibroblasts in cancer: a novel tumor-promoting cell type. *Cell Cycle* 2006, 5:1597–1601
4. Fusenig NE, Breitkreutz D, Dzarlieva RT, Boukamp P, Bohnert A, Tilgen W: Growth and differentiation characteristics of transformed keratinocytes from mouse and human skin in vitro and in vivo. *J Invest Dermatol* 1983, 81:168–175
5. Nyström ML, Thomas GJ, Stone M, Mackenzie IC, Hart IR, Marshall JF: Development of a quantitative method to analyse tumour cell invasion in organotypic culture. *J Pathol* 2005, 205:468–475
6. Gaggioli C, Hooper S, Hidalgo-Carcedo C, Grosse R, Marshall JF, Harrington K, Sahai E: Fibroblast-led collective invasion of carcinoma cells with differing roles for RhoGTPases in leading and following cells. *Nat Cell Biol* 2007, 9:1392–1400
7. Mueller MM, Fusenig NE: Friends or foes—bipolar effects of the tumour stroma in cancer. *Nat Rev Cancer* 2004, 4:839–849
8. Schäfer M, Werner S: Cancer as an overhealing wound: an old hypothesis revisited. *Nat Rev Mol Cell Biol* 2008, 9:628–638
9. Stewart EA, Friedman AJ, Peck K, Nowak RA: Relative overexpression of collagen type I and collagen type III messenger ribonucleic acids by uterine leiomyomas during the proliferative phase of the menstrual cycle. *J Clin Endocrinol Metab* 1994, 79:900–906
10. Kylmäniemi M, Oikarinen A, Oikarinen K, Salo T: Effects of dexamethasone and cell proliferation on the expression of matrix metalloproteinases in human mucosal normal and malignant cells. *J Dent Res* 1996, 75:919–926
11. Chang SE, Foster S, Betts D, Marnock WE: DOK, a cell line established from human dysplastic oral mucosa, shows a partially transformed non-malignant phenotype. *Int J Cancer* 1992, 52:896–902
12. Locke M, Heywood M, Fawell S, Mackenzie IC: Retention of intrinsic stem cell hierarchies in carcinoma-derived cell lines. *Cancer Res* 2005, 65:8944–8950
13. Mackenzie IC: Growth of malignant oral epithelial stem cells after seeding into organotypic cultures of normal mucosa. *J Oral Pathol Med* 2004, 33:71–78
14. Costea DE, Kulasekara K, Neppelberg E, Johannessen AC, Vintermyr OK: Species-specific fibroblasts required for triggering invasiveness of partially transformed oral keratinocytes. *Am J Pathol* 2006, 168:1889–1897
15. Riekkilä R, Parikka M, Jukkola A, Salo T, Risteli J, Oikarinen A: Increased expression of collagen types I and III in human skin as a consequence of radiotherapy. *Arch Dermatol Res* 2002, 294:178–184
16. Nyberg P, Heikkilä P, Sorsa T, Luostarinen J, Heljasvaara R, Stenman UH, Pihlajaniemi T, Salo T: Endostatin inhibits human tongue carcinoma cell invasion and intravasation and blocks the activation of matrix metalloproteinase-2, -9, and -13. *J Biol Chem* 2003, 278:22404–22411
17. Risteli L, Risteli J: Analysis of extracellular matrix proteins in biological fluids. *Methods Enzymol* 1987, 145:391–411
18. Risteli J, Elomaa I, Niemi S, Novamo A, Risteli L: Radioimmunoassay for the pyridinoline cross-linked carboxy-terminal telopeptide of type I collagen: a new serum marker of bone collagen degradation. *Clin Chem* 1993, 39:635–640
19. Opendakker G, Ashino-Fuse H, Van Damme J, Billiau A, De Somer P: Effects of 12-O-tetradecanoylphorbol 13-acetate on the production of mRNAs for human tissue-type plasminogen activator. *Eur J Biochem* 1983, 131:481–487
20. Airola K, Karonen T, Vaalamo M, Lehti K, Lohi J, Kariniemi AL, Keski-Oja J, Saarialho-Kere UK: Expression of collagenases-1 and -3 and their inhibitors TIMP-1 and -3 correlates with the level of invasion in malignant melanomas. *Br J Cancer* 1999, 80:733–743
21. Peebles PT, Trisch T, Papageorge AG: Isolation of four unusual pediatric solid tumor cell lines. *Pediatr Res* 1978, 12:485
22. Ramos-DeSimone N, Hahn-Dantona E, Siple J, Nagase H, French DL, Quigley JP: Activation of matrix metalloproteinase-9 (MMP-9) via a converging plasmin/stromelysin-1 cascade enhances tumor cell invasion. *J Biol Chem* 1999, 274:13066–13076
23. Coussens LM, Werb Z: Inflammation and cancer. *Nature* 2002, 420:860–867
24. Folkman J: Tumor angiogenesis: therapeutic implications. *N Engl J Med* 1971, 285:1182–1186
25. Shintani Y, Maeda M, Chaika N, Johnson KR, Wheelock MJ: Collagen I promotes epithelial-to-mesenchymal transition in lung cancer cells

- via transforming growth factor- β signaling. *Am J Respir Cell Mol Biol* 2008, 38:95–104
26. Potenta S, Zeisberg E, Kalluri R: The role of endothelial-to-mesenchymal transition in cancer progression. *Br J Cancer* 2008, 99:1375–1379
 27. Vihinen P, Kähäri VM: Matrix metalloproteinases in cancer: prognostic markers and therapeutic targets. *Int J Cancer* 2002, 99:157–166
 28. Borchers AH, Steinbauer H, Schafer BS, Kramer M, Bowden GT, Fusenig NE: Fibroblast-directed expression and localization of 92-kDa type IV collagenase along the tumor-stroma interface in an in vitro three-dimensional model of human squamous cell carcinoma. *Mol Carcinog* 1997, 19:258–266
 29. Korpi JT, Kervinen V, Mäklin H, Väänänen A, Lahtinen M, Läärä E, Ristimäki A, Thomas G, Ylipalosaari M, Åström P, Lopez-Otin C, Sorsa T, Kantola S, Pirlä E, Salo T: Collagenase-2 (matrix metalloproteinase-8) plays a protective role in tongue cancer. *Br J Cancer* 2008, 98:766–775
 30. Zober BL, Turner MA, Palefsky JM, Banda MJ, Kramer RH: Type I collagen degradation by invasive oral squamous cell carcinoma. *Oral Oncol* 2000, 36:365–372
 31. Koizumi M, Yamada Y, Takiguchi T, Nomura E, Furukawa M, Kitahara T, Yamashita T, Maeda H, Takahashi S, Aiba K: Bone metabolic markers in bone metastases. *J Cancer Res Clin Oncol* 1995, 121:542–548
 32. Bode MK, Mosorin M, Satta J, Risteli L, Juvonen T, Risteli J: Complete processing of type III collagen in atherosclerotic plaques. *Arterioscler Thromb Vasc Biol* 1999, 19:1506–1511
 33. Mäkelä JK, Raassina M, Virta A, Vuorio E: Human pro α 1(I) collagen: cDNA sequence for the C-propeptide domain. *Nucleic Acids Res* 1988, 16:349
 34. Vuorio T, Mäkelä JK, Kähäri VM, Vuorio E: Coordinated regulation of type I and type III collagen production and mRNA levels of pro α 1(I) and pro α 2(I) collagen in cultured morphea fibroblasts. *Arch Dermatol Res* 1987, 279:154–160
 35. Sandberg M, Mäkelä JK, Multimäki P, Vuorio T, Vuorio E: Construction of a human pro α 1(III) collagen cDNA clone and localization of type III collagen expression in human fetal tissues. *Matrix* 1989, 9:82–91
 36. Pihlajaniemi T, Tryggvason K, Myers JC, Kurkinen M, Lebo R, Cheung MC, Prockop DJ, Boyd CD: cDNA clones coding for the pro- α 1(IV) chain of human type IV procollagen reveal an unusual homology of amino acid sequences in two halves of the carboxyl-terminal domain. *J Biol Chem* 1985, 260:7681–7687
 37. Kallunki P, Sainio K, Eddy R, Byers M, Kallunki T, Sariola H, Beck K, Hirvonen H, Shows TB, Tryggvason K: A truncated laminin chain homologous to the B2 chain: structure, spatial expression, and chromosomal assignment. *J Cell Biol* 1992, 119:679–693